Shearing Conditions on the Interface of a Spherical Water Drop Sinking in Silicone Oil

Tomomasa Uemura
Department of Industrial Engineering, Kansai University, 3-35 Yamate-cho, Suita, Osaka 564-8680, Japan
Makoto Yamauchi
Department. Systems and Control Engineering, Osaka Prefectural College of Technology, 26-12 Saiwai-cho, Neyagawa, Osaka 572-8572, Japan

This paper deals with the experiment to obtain quantitative information about conditions of the interface between a water drop and surrounding oil. Velocity distributions in very close region of the interface are measured by introducing a new illumination technique and a telecentric lens. It enables precise measurements of velocity distributions in the close region to the interface. Although the measured velocity distributions exhibit strong influence from the solid wall of an experimental tube, the coincidence of inner and outside velocities on the interface is clearly confirmed for the clean interface. The shearing stresses on the interface, which are proportional to the velocity gradient normal to the interface, clearly show conditions of contaminated interface, which can be divided into two parts. From front stagnation point to somewhere near a separation point, the distribution of shearing stresses is well coincide with that of the Hadamard's analytical solution, while the distribution on the latter part of the interface shows quite different feature, which is supposed to be strongly influenced by contamination of the surface.

Key Words : Interfacial Slip, Contamination, PTV, Velocity Distribution, Liquid-Liquid Two -Phase Flow Nomenclature

Nomenclature

A : Projected area of a drop,
C_D : Coefficient of drag,
D : Drag force,
D_B : Diameter of a drop,
n : Coefficient of refraction between two liquids,
r : Radial distance from origin,
E_0 : Eotvos number,
R : Radius of a spherical drop,
R_e : Reynolds number,
V_θ : Tangential velocity along surface of a drop,
V_B : Sinking velocity of a drop,
x : Apparent vertical position,
X : Vertical distance from origin,
α : Angle measured from horizontal plane
ε : Correction factor,
ρ_c : Density of the continuous phase,
θ : Latitude angle measured from the front stagnation point,

* Corresponding Author.
E-mail : umra@kansai-u.ac.jp
TEL : +81-6-6368-0802; **FAX** : +81-6-330-3154
Department of Industrial Engineering, Kansai University, 3-35 Yamate-cho, Suita, Osaka 564-8680, Japan.
(Manuscript **Received** September 3, 2001; **Revised** October 16, 2001)

1. Introduction

The transport phenomena across the interface between dispersed and continuous phase have been interested in the field of multiphase flow. If reactions occurred across the interface were quantitatively known, total amount of any transported quantities can be estimated easily. However, no such information had been obtained,

so far. The most existing experimental data show the global flow condition of mixing or behaviors of dispersed phase.

Flow conditions at both sides of the interface play important role in the phenomena. Many researchers have been studied flow conditions in various multiphase flows, but most of experimental reports do not contain quantitative information about the interfacial conditions.

When a liquid drop moves in a continuous phase, the liquid inside the drop is driven by the outer flow through the interface. In order to estimate the amount of the transported momentum across the interface, the boundary conditions such as slip on the interface, the transportation factor, its distribution, and so on have to be known quantitatively.

Numerical analysis have been widely and successfully applied to predict and to estimate many fluid dynamic engineering problems. Two-phase flows have been one of the most suitable objects for numerical analysis. It has succeeded in predicting macroscopic phenomena such as behaviors of dispersed phase, mixing flows driven by bubble blowing, etc. In those analyses, boundary conditions on the phase-interface are given as averaged values obtained from macroscopic measurements, or are provided by some theoretical models. Such methods may be effective to confirm the similarity between known results and the numerical simulations in the sense of overall resemblance. In order to analyze or to estimate unknown phenomena, it is indispensable to know the transport phenomena actually occurred on the interface of the phases concerned.

Garner et al. (Garner, F. H. and Skelland, A. H. P. 1954) measured velocities inside a drop using quantitative visualization technique, and Kinter (Kinter, R. C. 1963) studied about the influence of contamination of the interface to the flow inside a drop. They observed the flow patterns and measured velocities by manually analyzing pictures. But, the data were not sufficient to examine flow conditions on the interface in both aspects of quantity and quality. Experimental measurement of transient and spatially distributed phenomena occurred in a moving space is not easy. But, whole field velocimetry techniques are suitable to measure such spatially distributed and transient phenomena, only if the phenomena are visually captured.

This paper aims to measure characteristics of the flow in the proximity of the liquid-liquid interface of a sinking water drop in silicone oil using a PTV technique. In order to measure the flow, pictures have to satisfy some important requirements such as clear tracer images up to the interface region, a distinct outline of the drop. And image distortions due to the spherical interface of a drop, should be corrected to measure the inner region of the drop. Some flow visualization techniques were developed to resolve the above requirements. There are some more issues to be considered in the experimental condition, such as influence of contaminations introduced by tracer particles, and influence of the surrounding wall on the flow.

The measured velocities clearly show the distribution of shearing stresses on the contaminated interface of a drop. Thin and non-slippery structure is detected on the surface. The structure immigrates from a nose to a rear of the drop. The behavior and physical characteristics of the skin-like structure are the origin of the wide variation in drag coefficients of dispersed phase. The experimental results show a part of the conditions of the skin as the surface friction material of a drop.

2. Experiments and Measuring Method

2.1 Experimental method and conditions

Figure 1 shows the experimental set-up, which consists of a cylindrical glass tube with inner-diameter 31-mm, a square water tank with transparent wall, a laser light sheet, and two high-resolution video cameras. The glass-tube is filled with silicone oil, of which kinematic viscosity is 1×10^{-4} [m^2/s] with a density of 976 kg/m^3 at 20℃.

A laser light sheet 2mm thick is applied from a normal direction to the observation axis, and the light illuminates the vertical and diametric cross

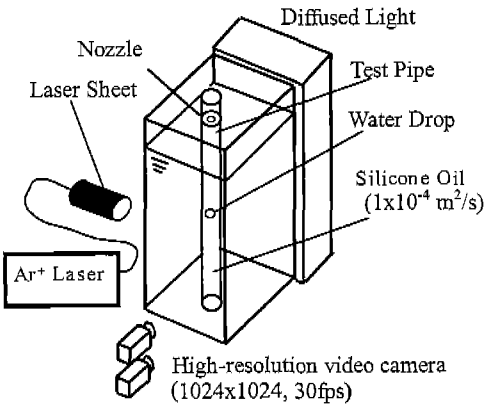

Fig. 1 Experimental apparatus

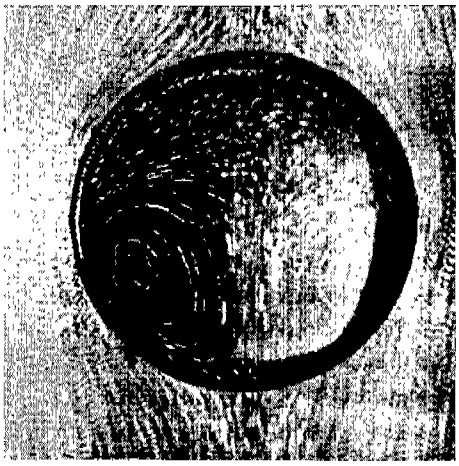

Fig. 2 Flow pattern around and inside the water drop *C* in Table 1

section of the sinking drop. The illumination visualizes tracer particles (spherical nylon particles with about 0.08mm average diameter) within the illuminated cross sectional plane. Since the image deformations under this optical condition are not heavy, the coordinates of apparent tracer images can be easily calibrated. Although no strong reflection from the interface occurs, the edge line of the drop, however, cannot be clearly observed. In order to make the outline clear, an additional illumination using a weak diffused light is applied from behind the object. Motions of the drop and tracer particles are captured at 30 fps using two high spatial resolution video cameras; one takes motion of a drop, and the other pictures a closeup scene of the drop. Pictureswith 1024×1024-pixels spatial resolution are directly transferred to computer memory. Figure 2 shows one of the instantaneous pictures taken under the illuminations. Since the refraction index of water is less than that of the silicone oil, a whole inner region of the water drop can be observed up to the inner boundary. In order to measure instantaneous velocity distribution around and inside the water drop, the PTV technique is effectively utilized.

In this experiment, the contamination is the primary factor governing the flow around the drop. Deionized water is used for the drop, and the water is carefully dribbled to a nozzle at the surface of silicone oil. A drop with a diameter around 12mm to 15mm is formed, and it goes downward in the vertical glass tube. Nylon spherical particles 0.08mm in diameter were premixed in the liquids as tracer for PTV. In order to keep the working fluids as clean as possible, the tracer particles are carefully washed using ethanol and deionized water beforehand.

Experimental conditions are set so that the drop sinks straight downward without fluctuation maintaining its spherical shape. Strictly speaking, the shape is actually an ellipsoid vertically flattened by about 2%. Velocity distributions are measured for water drops with three different contamination levels, each of which strongly influences the fluid drag of the drop. Generally speaking, experimental conditions have to be kept constant in every series of measurements.

2.2 Influence of contamination and finite cross sectional area

In the present experiment, since controlling the contamination level of the interface is almost impossible, contamination level are left as it goes on during a set of measurements are executed. The sinking velocity of the water drop gradually slowed down as the experiment is repeated under the same conditions. The sinking velocity is influenced by the contamination, shape and volume of the drop, and the pipe diameter. The slower velocity seems to be caused by deteriorated fluids, because all other influencing factors are

kept constant. No matter how tracers are carefully washed, the reduction of the sedimentation velocity occurs similarly in the case without tracers. It is confirmed that the sedimentation velocity of a water drop decreased while repeating the experiment irrespective of the presence of the tracer particles.

Generally speaking, contamination levels have to be measured quantitatively; there is no quantitative definition to establish its scale. Controlling the contamination level is also very difficult. The sedimentation velocity has been used as a convenient index of the degree of contamination. However, it is inadequate to express the degree of contamination by the sedimentation velocity itself without the comparative standard value. In this paper, the coefficient of drag is employed as a measure of the contamination level, since it is non-dimensional and applicable to compare it with the established data.

The sedimentation velocity of a drop and velocity distributions are measured under various contamination levels, which happen during repeated use of experimental fluid.

The coefficient of the fluid drag is utilized as an index of the degree of the contamination. The non-dimensional coefficient is more suitable than the sedimentation velocity to index the contamination level, because it is free from the influence of the drop diameter. The coefficient can be evaluated easily from the drop's velocity and diameter of the drop. The coefficient is defined as follows:

$$D=C_D A\frac{\rho_c V_B^2}{2} \tag{1}$$

In Eq. (1), D is drag force, which equals to the sedimentation force, V_B is the sedimentation velocity, A is a projection area of the drop, and ρ_c is the density of the continuous phase.

The experimental condition is summarized in Table 1 where D_B is a horizontal diameter of a drop, V_B is a sedimentation velocity, Re and C_D are Reynolds number and a coefficient of drag, respectively. The flow pattern in Fig. 2 corresponds to the experimental condition 'C' in Table 1.

As seen in the table, the sedimentation velocity and the coefficient of the fluid drag are changed, while the diameter of the drop varies a little. It should be referred that those values of the coefficients are fairly large comparing to the theoretically estimated values. The C_D's shown as 16/Re is considered for a liquid drop with boundary condition when the inner and outer velocities coincide on the interface. And, the $C_D=24/Re$ corresponds to the Stokes flow for the solid sphere with a non-slip surface. The experimental values are expected to be in between the two values. Such large C_D's values are caused by the finite cross sectional area of the experimental tube. The ratio of the drop diameter to the inner diameter of the tube is around 0.5 for the present experiments. When a water drop with about one half diameter of a glass tube moves down in silicone oil in the tube, the displaced oil has to moves upward and the motion cause extra resistance to the drop.

Table 1 Experimental conditions

	D_B(mm)	V_B(mm/s)	Re	C_D	Theoretical C_D	
					$16/Re$	$24/Re$
A	15.4	17.6	2.7	23	5.9	8.9
B	14.6	11.5	1.7	50	9.4	14.1
C	15.6	9.4	1.5	80	10.7	16

This effect increases the upward velocities especially in the vicinity of the drop. In other words, the sedimentation velocity of the drop becomes slower than that in the infinite space, or the drag coefficient looks larger than that of Stokes.

In the reference of Clift and Grace (1978), under the present experimental conditions, C_D's can be more than five times larger than the theoretically estimated values.

The main target of the present experiments is to capture the phenomena occurred at the interfacial region, especially, the velocity distribution and slip on the interface. The values of sedimentation velocity will not be discussed in detail in this paper, since the wall effects on the drop will not alter the phenomena.

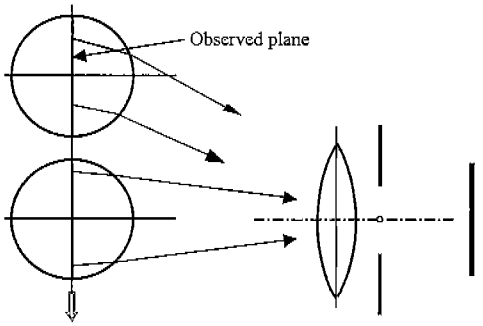

Fig. 3 Effects of refraction at spherical surface and a perspective deform the observation plane inside a drop

2.3 Velocity measurement inside a drop

The two circulating flows in Fig. 2 are the cross sectional view of one annular ring convection flow, which is driven by the external shearing force. The shearing stress on the inner surface can be evaluated from the inner velocity gradients, only if the velocities are obtained by analyzing a series of pictures using PTV. The picture contains distortions, which is caused by spherical surface of the drop, circular cylindrical wall of the tube, and the camera lens. Among those distortions, the first one is the most complicated as explained below. The vertical and central plane of a drop is illuminated for observation. When the observation plane inside a drop moves across the view field, optical paths to form an image change simultaneously as shown in Fig. 3.

Under such optical condition, the image distortion is a function of the curvature of the drop surface and locations in the view field. Adding to the difficulty, the distortion is significant at interfacial region, where the velocities have to be measured as precisely as possible. In order to solve the problems, a telemetric lens, which portrays objects using only rays parallel to the lens axis, is utilized to picture the observation plane of a drop. The optical paths from the observation plane to the image sensor become substantially simple in this method as shown in Fig. 4, and the relationship between the actual position in the observation plane and the apparent position is shown as Eq. (2) for a spherical drop, which is obtained by considering

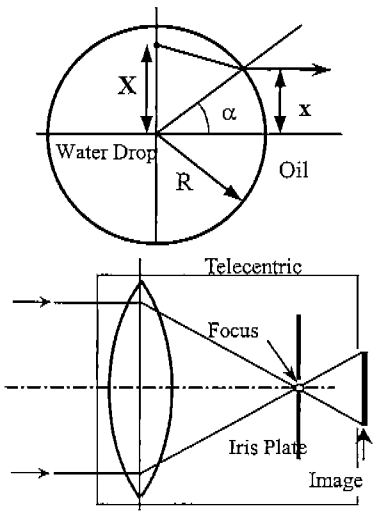

Fig. 4 Refraction of a ray at a water drop surface in oil in a telecentric lens imaging condition

only parallel rays to the lens axis. The correction factor to be multiplied to the apparent position in the plane is X/x in the figure.

$$X=\frac{x}{\sqrt{n^2-\sin^2\alpha}\cdot\cos\alpha+\sin^2\alpha} \qquad (2)$$

In the present experiment, the refraction index of silicone oil is $n_o=1.403$, and that of water is $n_w=1.333$. 'n' in the above equation is the relative refraction index ($=n_w/n_o$). The ratio X/x is nearly constant ($=1.05$ to 1.065) within the most cross sectional region except the peripheral interfacial zone, as a result.

The shape of the drop is actually a vertically flattened ellipsoid by about 2%. In that case, the similar Eq. (3) can be applied, and it is confirmed that the differences from Eq. (2) are small. The 'ε' in Eq. (3) is a correction factor due to the aspect ratio of the ellipse.

$$X+\varepsilon=\frac{x+\varepsilon}{\sqrt{n^2-\sin^2\alpha}\cdot\cos\alpha+\sin^2\alpha} \qquad (3)$$

3. Velocity Distributions Near And Both Sides Of The Interface

3.1 Flow inside a water drop

Figure 5 shows mean velocity distribution measured at the interface region of a drop sinking

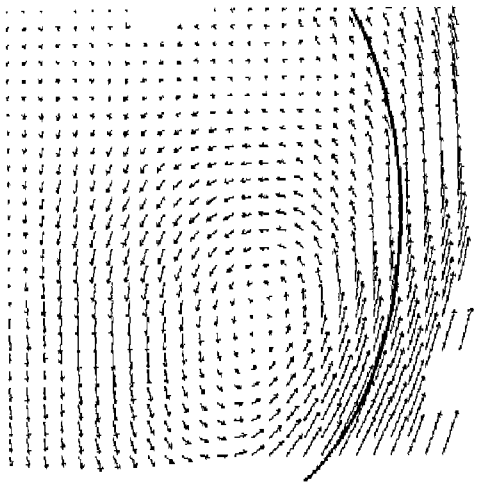

Fig. 5 Velocity distribution measured in the side region of a water drop

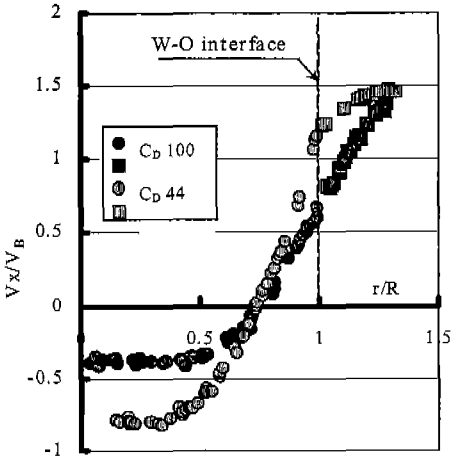

Fig. 6 Distributions of vertical velocities along a horizontal axis of a drop

in oil. The distribution is obtained from randomly distributed velocity vectors. The randomly distributed vectors are interpolated to regular grid points, and then averaged. Figure 6 shows the vertical velocity along the horizontal axis of a drop. At the water-oil interface (r/R= 1), the velocity gradient for C_D=44 changes abruptly, while the distribution for C_D=100 changes a little. But, when considering that the viscosity of the oil is 100 times larger than that of water, the difference of shearing stresses between the both sides of the interface is larger in the latter

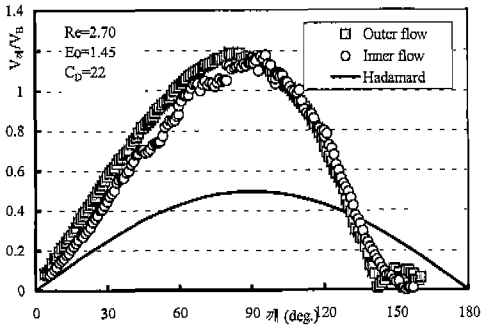

Fig. 7 Comparison of velocity distributions measured from 0.1mm inside and outside the interface of a sinking water drop

case. The velocity gradient across the interface is discontinuous, while velocities are continuous. This suggests that the boundary condition assumed by Hadamard is valid.

A flow inside a water drop can be observed up to the close vicinity of the inner surface, since the refractive index of water is less than that of silicone oi. A pair of circulations is observed in Fig. 2. They provide a cross sectional view of one spherical vortex. A dead water zone exists in the upper the drop. The dead water region occupies wider area as the C_D value increases. The circulation zone is pushed downward. The displacement is caused by the accumulation of the contamination agent at the upper part of the interface, where the concentrated agent hardens the interface, and it insulates the inner fluid from the influence of outer conditions. This raises the question as to the changes of the skin conditions along the surface from the front stagnation point toward the rear one. A part of the answer could be obtained by comparing velocity distributions measured inside and outside of the drop.

3.2 Flow along the interface

Velocity distributions along the interface for C_D=22 are shown in Fig. 7. Velocity distributions measured on both sides of the interface and that of the Hadamard's solution are compared in the figure. The large difference between the experimental results and the theoretical distribution occurred mainly by the finite cross section of the experimental tube, as mentioned in Sec. 2.2.

The two adjacent flows to the interface exhibit almost the same velocity distributions from $\theta=0$ up to 130 degrees, where the inner velocities slightly lower than the outer ones. The flow along the inside interface is asymmetric. The two velocities on each side of the interface well coincide from the nose up to 120 degrees. And the both distributions are not symmetric with respect to $\theta=90$ degrees. Between $\theta=110$ and 120 degrees, the outside velocity temporally becomes lower than the inside velocity. In the region with $\theta>=$ 120 degrees, fluids inside the drop moves slowly and independently from the outside flow. Considering these conditions, the contamination skin covers this regions, and it becomes thicker from $\theta>=100$ degrees. The boundary conditions for the analysis have to be different from the front sides. For a more detailed understanding of the skin's characteristics, the velocity gradient on its surface has to be examined more precisely.

3.3 Shear along the interface

The changes of the physical condition on the interface are not found clearly in the velocity distributions in Fig. 7. The radial gradient of the circumferential velocity component on the interface corresponds to the shearing stress. The velocity gradient can be estimated by interpolating randomly distributed PTV data. One example of the distribution of the velocity gradient is shown in Fig. 8. Comparing to the velocity distributions shown in Fig. 7, velocity gradients tremendously well coincide with the prediction of the Hadamard's solution in the range from the front nose (lower end) up to 120 degree towards the rear end of the drop. This is because the velocity gradient is calculated by subtracting the neighboring velocities, acceleration effect by the surrounding wall seems to be canceled by the subtraction. Alternatively, the subtraction degrades the precision of the results.

The radial gradient in the range $\theta>120$ degree abruptly jumped up then fell down to zero forming a sharp peak. The rising part implies that the surface abruptly change its nature from slippery one to a solid. The region of the decreasing gradient corresponds to the wake region.

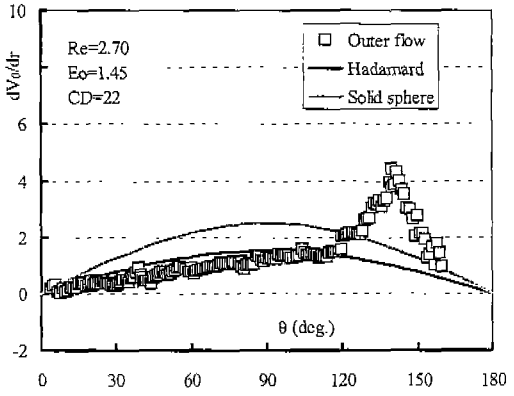

Fig. 8 The radial velocity gradient are compared with those theoretical solutions. In $\theta>120$, experimental results exhibit a peculiar feature

4. Conclusions

(1) Velocity distributions inside and outside of a water drop sinking in oil were measured up to close proximity of the interface.

(2) Velocities on both sides of the interface coincide in the range except wake region. In the wake region, the two flows are similar, but they behave independently.

(3) The radial gradients of circumferential velocity on the interface are evaluated, and a peculiar features was found.

Acknowledgements

Authors would like to appreciate to the financial support offered by the Kansai University through the Special Research Funds 2000 program, and also by the Kansai University Grant-in-Aid for the Faculty Joint Research Program, 2000. And authors also wish to express their acknowledgement referring that some instruments used in the study are purchased by the fund of the Grant-in-Aid for Scientific Research (C) No. 12650127.

References

Clift, R., Grace, J. R., and Weber, M. E., 1978, "Bubbles, Drops, and Particles," Chap. 9 Wall

Effects, Academic Press, pp. 221~243.

Garner, F. H., Skelland, A. H. P., Haycock, P. J., 1954, "Speed of Circulation in Droplets," *Nature*, p. 1239.

Kintner, R. C., 1963, "Drop Phenomena Affecting Liquid Extraction," *Advances in Chemical Engineering 4*, Academic Press, pp. 51~94.